DEVELOPMENT OF A NUMERICAL MODEL OF THE 9 MM PARABELLUM FMJ BULLET INCLUDING JACKET FAILURE

Ch. M a r é c h a l [1)], F. B r e s s o n [2)], G. H a u g o u [1)]

[1)] **Université Lille Nord de France**
F-59000 Lille, France
UVHC, LAMIH
F-59313 Valenciennes, France
CNRS, FRE 3304
F-59313 Valenciennes, France

[2)] **Institut National de Police Scientifique**
Laboratoire de Police Scientifique de Lille
7 bd Vauban, 59000 Lille, France

Even though ballistic experiments are widely accepted as the only reliable way to probe terminal effects, we demonstrate that computer simulation can be a useful alternative. Particularly, the high energy projectiles are seldom studied in the field of forensic sciences. That situation being favorable to computer simulation, a 3D finite element model of the worldwide-used 9 mm Parabellum bullet has been developed with Abaqus explicit software. A Johnson-Cook constitutive model, fed with the split Hopkinson pressure bar experimental parameters, accurately describes the materials' behavior (lead and brass). Experiments were performed with a handgun and a hard steel plate target in order to discuss the reliability of the model. Accurate predictions about bullet deformation and failure were obtained without any post-calculation adjustment of parameters.

Key words: ballistics, FEM, Johnson-Cook.

1. Introduction

Gunshot investigation is a key activity of any forensic science institute. The shooter's position is classically estimated from a post impact examination of a scene (multiple impacts). The line passing by the center of each impact figure is materialized with a laser beam or a set of metallic rods. It can also be calculated from an accurate 3D positioning of each impact. A correction of the bullet's path deflection (under the influence of its weight) can be considered in some particular cases (long distance shooting). As a consequence, if a gunshot involves only a single impact no information about the position of the shooter can be given. The second limitation is the lack of knowledge about impact

phenomena (deflection, velocity loss, bullet's integrity and stability) which are known qualitatively but not quantitatively. A specific procedure involving target examination (gunshot residue scattering, smoke or multi-projectile dispersion, the Griess test) is also applied to estimate the shooting distance (not the angle), but besides the specific case of shotgun (multi-projectile), the efficiency range of these methods is typically limited to a few meters.

In that context, it has already been demonstrated that comparing the bullet deformation with experiments can bring up some information about the shooting distance, in the case of a hard target (metal, concrete [1]) or a soft target (human body [2, 3]). The method used to determine the ballistic parameters is the experimental way, the main reason being the lack of adequate computer simulation of material deformation in the ballistic domain. The source of this inadequetness can be found in the complexity of the problem itself, and also in the low number of applications. The deformation state under ballistic impact velocities (from 100 to 1000 ms^{-1}) can only be described by rather complex and multi-parameter laws. Identifying each parameter is a problem, the complexity of which increases with the impact velocity. The ballistic domain stands between the Lagrangian (solid) and Eulerian (fluid) formulation. Unifying these formulations is still an issue. On the application side, military requirements (effects of a given structure of projectile hitting a given structure of target) are quite easy to investigate with experimental tools. In forensic applications (recovery of pre-impact information from post impact examination), computer simulation could be an alternative to experiments when a gunshot cannot be accurately reproduced (excessive distance, accuracy or cost), but this demand was only formulated lately.

In the present study, the worldwide- used 9 mm Parabellum FMJ (Full Metal Jacket) bullet was selected as a representative sample. A 3D finite element model has been developed with Abaqus explicit software. The constitutive model for lead and brass is based on the Johnson-Cook relation without failure formulation. The split Hopkinson pressure bar experimental data were used to identify the missing parameters. The predictions were compared with ballistic experiments performed with a semi-automatic Glock 26 compact pistol and homemade ammunition with muzzle velocity ranging from 30 to 200 ms^{-1}.

2. Ballistic experiments

The thrower is a Glock 26 semi-automatic pistol. The target is a 30 mm thick iron plate. The shooting distance is set to 2 m. Different velocities were obtained by varying the amount of propellant (Vectan Ba 9) in home-made 9 mm Parabellum cartridges. The bullets are 9 mm Parabellum lead core FMJ weighting 115 gr (grain), i.e., 7.45 g (actually ranging from 7.39 to 7.49 g in our

experiments). Impact velocities are measured half way between the handgun and the target with a chronograph (Pro Chrono, Competition Electronics Inc, USA). Very low velocities (down to 60 ms^{-1}) were repeatedly obtained.

The way we chose to describe both the length reduction and diameter expansion was to define a deformation criteria C as follow:

$$(2.1) \qquad C = \sqrt{\frac{1}{2} \cdot \left[\left(\frac{\Delta l}{l_0} \right)^2 + \left(\frac{\Delta d}{d_0} \right)^2 \right]},$$

with $\Delta l = l - l_0$ and $\Delta d = d - d_0$. l_0 and d_0 are respectively the length and the diameter of the bullet before impact. The nature of C (single value) is more suitable for comparison. This criteria can theoretically be higher than 1.

For each experiment, the length (l) and the diameter (d) of the bullet were measured using a micrometer and finally C was calculated. The behavior of C versus impact velocity is given in Fig. 1. The blue dots are the experimental data; the red lines are the least square approximation in the two distinctive areas. In the second area, the last two dots have not been considered for the least square approximation as they demonstrate a saturation behavior slightly below fragmentation.

Figure 1 demonstrates that C follows two rather linear behaviors, with a velocity threshold triggering jacket fracture in-between. The so-called frac-
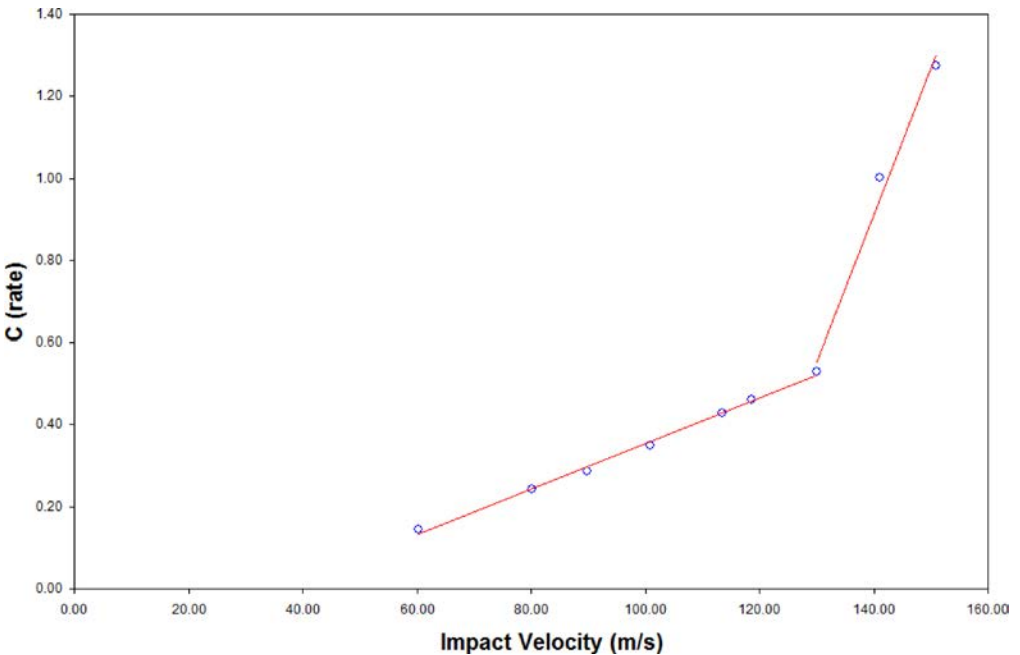

FIG. 1. Behavior of C versus impact velocity.

ture threshold is 130 ms^{-1} in the experimented case. The slope of the curve is $5.6 \cdot 10^{-3}$ sm^{-1} below the fracture threshold. Beyond the fracture threshold, the slope of the curve is 6 times higher $(3.4 \cdot 10^{-2}$ sm$^{-1})$ before reaching a saturation behavior and then approaching the fragmentation threshold. A core fragmentation has been observed with an experimental impact velocity of 176 ms^{-1}. Core and jacket fragmentation has been observed with an impact velocity slightly higher (182 ms^{-1}). This area cannot be described with C. With an impact velocity of 203 ms^{-1}, a part of the core remained soldered to the target. Beyond the fragmentation threshold, the size of the fragments decreases as the velocity increases. We believe, however, that a very little quantitative prediction can be gathered from a statistical fragment sizing.

Table 1 exhibits the shape of the deformation and eventually a fracture and fragmentation of few bullets for impact velocities ranging from 60 to 200 ms^{-1}.

Table 1. Deformation shape, fracture and fragmentation of the projectile for various impact velocities.

Impact Velocity [ms^{-1}]	60	80	101	119	141	164	182	203
C (rate)	0.14	0.24	0.35	0.46	1	1.46		

The experimental fracture and fragmentation speed thresholds will increase dramatically when the target cannot withstand ballistic load without deformation, as in most of the forensic cases. In that situation, any new target, new material or new target shape actually need a new study, pointing out to the usefulness of a FEM simulation tool.

3. FEM MODEL

3.1. Materials models

This part describes the determination of the mechanical properties of the quasi-pure lead extracted from the bullets by heating process ($\rho = 11300$ kg m^{-3} and $\nu = 0.42$). The purpose is to determine the true plastic laws from quasi-static to dynamic loadings under compression loading. Finally, parameters of the constitutive simplified Johnson-Cook model are calculated without considering heat transfer, as shown in Eq. (3.1) [4].

$$(3.1) \qquad \sigma = (\sigma_0 + K \cdot \varepsilon^n) \times \left(1 + D \cdot \ln\left(\frac{\dot{\varepsilon}}{\dot{\varepsilon}_0}\right)\right),$$

σ_0 is the yield stress, K is the hardening parameter, n is the exponent for the static law and D is the parameter which determine the viscosity effects. $\dot{\varepsilon}_0$ describes the activation of the strain rate effects.

The experimental setup includes the cylindrical samples ($\varnothing = 8$ mm, $l_0 = 7$ mm) submitted to the compression loadings from:

- A high-speed hydraulic machine (VHS) with a strain rates ranging from 0.15 to 20 s^{-1} (Fig. 2a),
- A set of nylon split Hopkinson pressure bars with a strain rate ranging from 800 to 2000 s^{-1} (Fig. 2b).

a)   b)

FIG. 2. a) VHS setup, b) Hopkinson bars setup.

Figure 3b illustrates the behaviour of the considered materials used for the determination of the Johnson-Cook parameters. The materials responses are determined from:

- strain gauges for Hopkinson tests,
- piezoelectric load cells coupled with electro-optical extensometers for VHS tests.

The raw signals have been recorded using a numerical recorder at adaptive sampling rates. For the Hopkinson calculations, the visco-elasticity and punching corrections have been considered [5, 6].

The Johnson-Cook parameters have been determined after keeping plastic relations at 0.15, 20800 and 1500 s^{-1} (dotted line in Fig. 3b). A classical calculation based on least squares interpolation has been used. The results are sum up in Table 2.

Lead has revealed a visco-elasto-plastic behaviour under compression loadings, but the authors have considered only visco-plasticity as a first step.
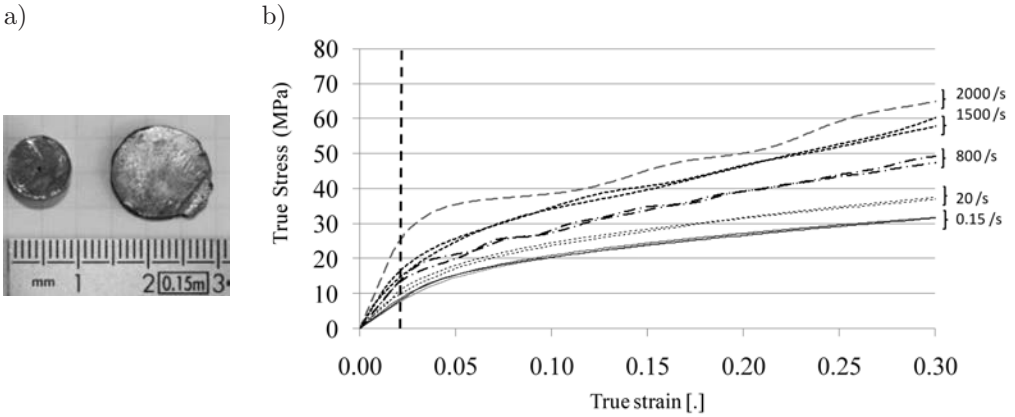
a)

b)

Fig. 3. a) Initial and final shapes of specimens; b) behaviour laws under compression loadings from 0.15 to 2000 s^{-1}.

Table 2. Johnson-Cook parameters for lead samples ($R^2 = 0.9891$).

E_{STATN}	E_{DYN}	σ_0	K	n	D
0.41 GPa	1.3 GPa	5.15 MPa	35.35 MPa	0.5	0.0628

3.2. Numerical model

The numerical simulation was developed by Abaqus finite element model software with the explicit numerical algorithm formulation. The projectile and the target were designed using a 3D axi-symmetric solid model. The impact has been considered as an axi-symmetric phenomenon by neglecting spinning effects of the projectile (spinning energy represents only few percent of the total kinetic energy). Furthermore, bullets didn't undergo any twisted deformation in the experiments. The main interest of the axi-symmetric simulation was to save computation time without decreasing the accuracy.

The bullet was meshed in 4 nodes elements with reduced integration. The projectile grid is composed of 6000 elements. The mechanical behaviour of the projectile is the main issue of the simulation as the steel target has been considered as a pure elastic solid ($E = 210000$ MPa, $\rho = 7800$ kg m^{-3}, $\nu = 0.33$). The shape of the bullet was extracted from of picture of a cut-off bullet by a Matlab routine. Figure 4 presents the finite element model of the bullet (b) and the picture of the cut-off bullet (a).

The bullet design includes two materials: a lead core and a brass jacket (a copper alloy also known as tambac, 90% Cu and 10% Zn). A Johnson-Cook constitutive model has been used for each component. The parameters of lead are given in Table 2. The parameters of tambac are extracted from the literature [7, 8]. The model didn't include fracture, but the fracture threshold criterion

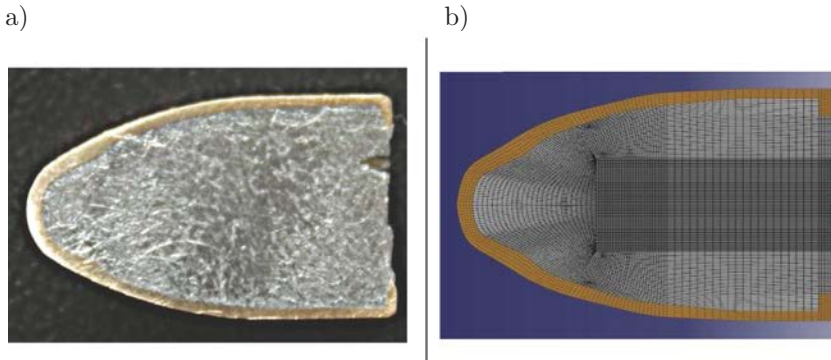a)   b)

FIG. 4. Cut-off picture (a) and FEM (b) of the bullet.

proposed by COCKCROFT and LATHAM [9] has been compared to the maximum load observed at the experimental fracture threshold (130 ms^{-1}). We also made sure that the plastic work, Wp, level overlaps the critical value proposed by BØRVIK *et al.* [10] for the brass jacket (Wp = 914 MPa).

Contact was considered without friction between the target and the bullet. Sliding was allowed between the lead core and the brass jacket, according to the experimental observations presented in Fig. 5.
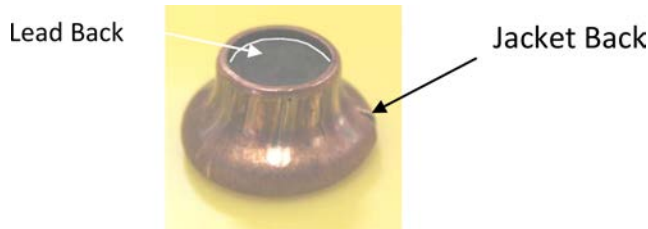

FIG. 5. Sliding between lead and jacket.

3.3. Correlation with experimental investigation

The model was run with velocities ranging from 60 to 160 ms^{-1}. The displacement and plastic work data were monitored from impact time (t) to $t + 3$ m/s (until the bullet reaches its steady post-impact state). Bullet diameter and length were extracted to calculate C for each simulation. Table 3 and the Fig. 6 show the results.

The numerical model and experimental results show a very good similarity until an impact velocity ranging from 130 to 140 ms^{-1} occurs. The experimental data exhibited fracture triggering at the same velocity. The fracture, allowing stress relaxation in the jacket, can not be considered in the model (not allowed in the axi-symetric configuration). Such a structural weakening increases crushing and the criterion C. The lack of stress relaxation in the model explains the

Table 3. Experiment and numerical results.

Experiments				Numerical				
Velocity [ms^{-1}]	Diameter [mm]	Length [mm]	C	Velocity [ms^{-1}]	Diameter [mm]	Length [mm]	C	WpMax [MPa]
60.3	9.46	11.23	0.14	60	9.08	11.67	0.15	478
80.2	10.8	10.10	0.24	80	10	10.18	0.21	484
89.9	11.35	9.73	0.29	100	11.3	8.7	0.32	447
100.9	12.1	9.12	0.35	120	12.36	7.62	0.42	614
113.4	13.05	8.45	0.43	130	12.9	7.08	0.47	687
118.6	13.4	8.08	0.46	140	13.54	6.5	0.52	2380
130.1	14.2	7.47	0.53	160	14.13	6.03	0.57	5586
141.1	20	4.3	1					
150.9	23.50	3.22	1.27					
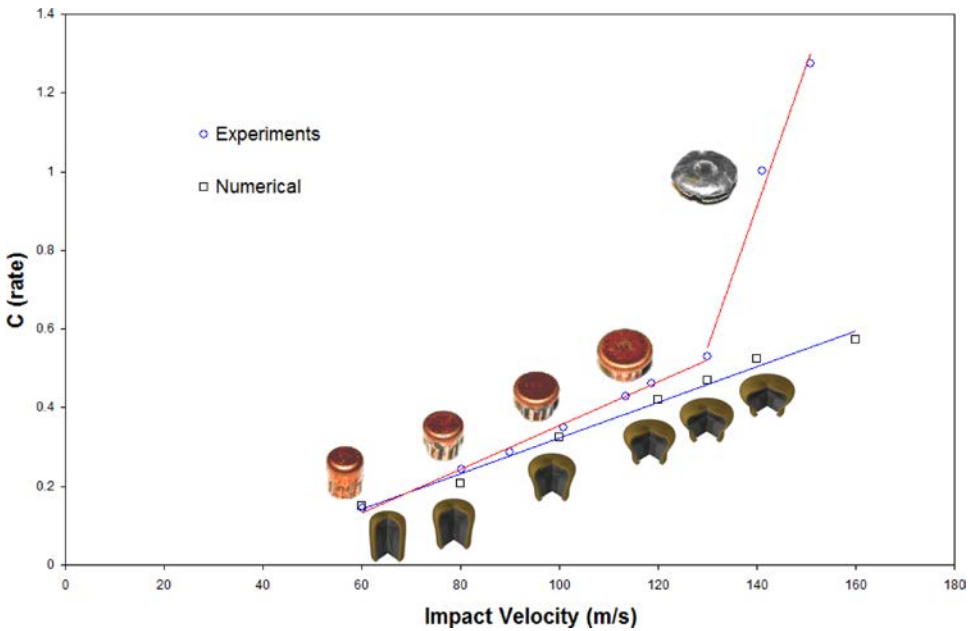
FIG. 6. Experiment and numerical behavior of C versus impact velocity.

difference between the experimental and the numerical results beyond 130 ms^{-1}. As explained above, the plastic work level has been used as an evidence to point out the emergence of fractures in the model. Figure 7 shows the evolution of the maximum plastic work of the jacket versus an impact velocity. The Børvik threshold criterion was overlapped with an impact velocity of 130 ms^{-1}. The non-linear increase of the plastic work is not realistic because of the enactment

of element in the model when the fracture phenomena appear. Modifications of the loading mode were observed in the model between 130 and 140 ms^{-1}. The jacket, which was in compression until 130 ms^{-1}, changed into a buckling mode. This change explains the fracture's triggering and the very important plastic work increase (according to a plastic strain increase). The agreement with experimental data is also very satisfactory.
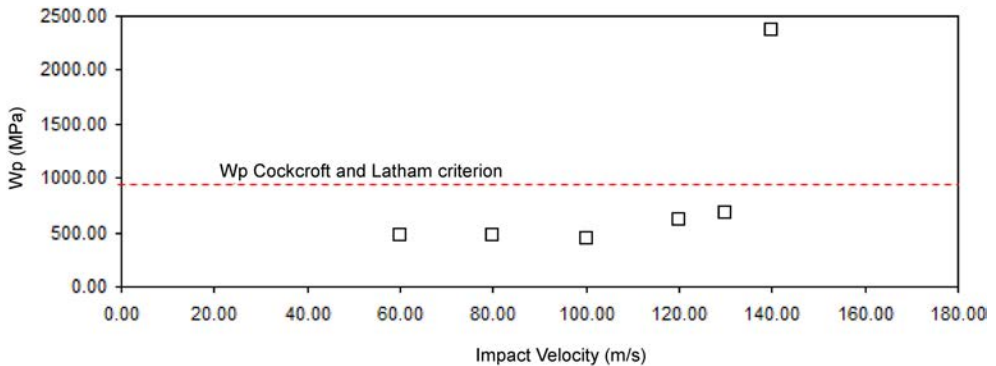

FIG. 7. Numerical results for maximum plastic work versus impact velocity.

Extra simulations (not reported here) demonstrated that a particular care must be taken about the jacket thickness variations. A maximum thickness is clearly visible near but off the tip (c.f., Fig. 4a). The approximation of a uniform thickness or even a slightly wrong shape induces a dramatic discordance with the experimental results.

4. CONCLUSIONS

This paper demonstrates the good correspondence between the FEM model using explicit formulation and the experiment in the ballistic field. The sine qua non condition for such a good behavior of the model was to provide accurate parameters for the Johnson-Cook constitutive model of each component. The parameters were extracted from the literature for tambac, from the Hopkinson bar experiments for the lead, and no extra adjustment were made. In that drastic situation, a very good concordance has been observed as far as the dynamic load did not exceed the fracture threshold.

For the explored velocity range, it has not been necessary to consider spin and heat transfer, but the results pointed out that a very good care about the jacket thickness is necessary to accurately reproduce the shape of the experimental deformations. Ongoing researches will include fracture and heat transfer in order to minimize the limitation of the Lagrangian formulation in the ballistic domain.

Acknowledgment

References

1. F. BRESSON, O. FRANCK, *Estimating the shooting distance of a 9 mm Parabellum bullet via ballistic experiment, Forensic Science International*, **192**, 1–3, 17–20, 2009.

2. K. G. SELLIER, B. P. KNEUBUEHL, *Wound ballistic and the scientific background*, Elsevier 1994.

3. F. BRESSON, O. FRANCK, *Comparing ballistic wounds with experiments on body simulator*, Forensic Science International, **198**, 1–3, 23–27, 2010.

4. G. R. JOHNSON, W. H. COOK, *A constitutive model and data for metals subjected to large strains, high strain rates and high temperatures*, Proceedings of seventh international symposium on ballistics, The Hague, the Netherlands, 1983.

5. G. GARY, V. DEGREEF, David, *Labview Version, Users manual version, LMS Polytechnique*, Palaiseau, 2008.

6. K. SAFA, G. GARY, *Displacement correction for punching at a dynamically loaded bar end*, International Journal of Impact Engineering, **37**, 4, 371–384, 2010.

7. S. CHOCRON, C. E. ANDERSEN Jr, D. J. GROSCH, C. H. POPELAR, *Impact of the 7.62 mm APM2 projectile against the edge of a metallic target*, International Journal of Impact Engineering, **25**, 23–37, 2001.

8. C. E. ANDERSEN Jr, M. S. BURKINS, J. D. WALKER, W. A. GOOCH, *Time-resolved penetration of B4C tiles by the APM2 bullet*, Computer Modeling in Engineering & Sciences, **8**, 2, 91–104, 2005.

9. M. G. COCKROFT, D. J. LATHAM, *Ductility and the workability of metals*, Journal of the Institute of Metals, **96**, 33–39, 1968.

10. T. BØRVIK, S. DEY, A. H. CLAUSEN, *Perforation resistance of five different high-strength steel plates subjected to small-arms projectiles*, International Journal of Impact Engineering, **36**, 7, 948–964, 2009.